A Variable Angle Slant-Hole Collimator

Richard H. Moore, Nathaniel M. Alpert, and H. William Strauss

Massachusetts General Hospital, Boston, Massachusetts

A variable-angle slant-hole (VASH) collimator was constructed to show the feasibility of using multiple sliding plates to achieve a range of collimator channel inclinations. One hundred and sixty tungsten plates, 0.125 mm thick and 14 cm square, were photoetched to produce 3025 1.5-mm^2 holes in each plate, separated by 0.8-mm septa. Along with the collimator holes, registration holes and positioning grooves were also etched. The plates were placed in a holder and stacked to form a collimator 2.0 cm high. The holder permitted the plates to be "sheared" to achieve viewing angles from 0 to 40° from the vertical. Resolution and sensitivity were determined both across and along the shear directions. Resolution of a thin Tc-99m source, 1.24 mm diam and 7 cm long, located 5 cm from the collimator face in air, was 1.1 cm FWHM at 0° shear and remained unchanged with increasing slant. The resolution was similar both across and along the shear plane. Sensitivity was determined with a point source placed 7 cm from the collimator face. At 0° slant the sensitivity was 169 cps/MBq (6.24 cps/μCi). A general all purpose (GAP) collimator had a FWHM of 1 cm for the line source in air at 5 cm, and a sensitivity of 205 cps/MBq (7.58 cps/μCi) for the point source at 7 cm. The data suggest that a variable-angle slant-hole collimator can be constructed of laminated plates.

J Nucl Med 24: 61–65, 1983

Parallel-hole collimators for scintillation cameras are typically constructed by casting, by packing tubes in an array, or as a joined series of foils (*1,2*). These collimators are fixed in the angulation of their holes, although some may be rotated to permit viewing of the object from several perspectives, or for limited-angle tomography of the heart (*3–10*) and other organs as suggested by Royal (*11*) and Pavel (*12*).

Chang et al. have strongly advocated that the axis of rotation used in rotating slant-hole (RSH) tomography be carefully aligned with an organ's long-axis centerline. They report artifacts in phantom studies when axial misalignments exceed 15° (*13–15*). Unfortunately for cardiac visualization, the anterior plane of most patients is not aligned with the long axis of the heart. Thus there may be some advantage to a technique that "decouples" collimator positioning from collimator viewing angle. In addition, the fixed-angle collimator design may not permit optimization of both collimator positioning (allowing the detector to be placed as close as possible to an object) and view angle.

To improve the relationship of the collimator to the object, while maintaining the desired view, we have designed and built a prototype collimator that permits the angle of slant to be varied easily by the operator. The collimator is composed of a series of tungsten plates that can be "sheared", as with a deck of cards, to adjust the angle of view. This report describes the construction and testing of this collimator.

METHOD

The collimator was designed to provide resolution and sensitivity similar to that of current "all-purpose" low-

June 21, 1982; revision accepted Oct. 1, 1982.

For reprints contact: H. William Strauss, MD, Nucl. Med. Div., Massachusetts General Hospital, Boston, MA 02114.

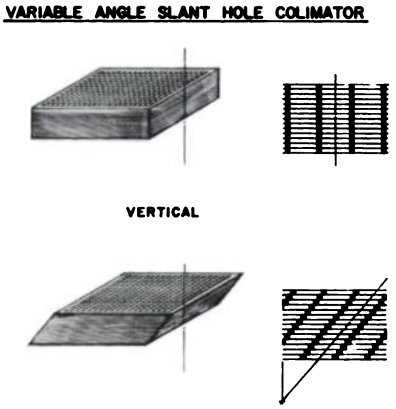

FIG. 1. Schematic cross section of VASH showing septal alignment and hole characteristics.

energy collimators and the additional ability to change continuously the angle of slant from vertical to 40° away from vertical (Fig. 1). The collimator was constructed of 160 tungsten plates, each 0.125 mm thick, aligned to form a stack 2.0 cm in height. The plates were fabricated by the photo-etch machining method. To do this, each tungsten plate, 14 × 14 × 0.125 mm, was coated with a light-sensitive material. A negative photographic mask of the collimator's septal pattern and alignment grooves was then exposed on the sensitized plate. The photosensitive material on the plates was developed, and the areas to be etched were rinsed from the soft, unexposed "photoresist" material. The plates were next sprayed with a corrosive acid solution that dissolved uncoated areas, leaving the residual metal in the pattern of the photoresist. This process cut 3025 regular 1.5-mm square holes separated by 0.8 mm septal bars into each plate. Figure 2 is a closeup photograph of a representative section, demonstrating the typical hole shape and border characteristics of sharp edges, mild surface undercut, and highly regular shape. The alignment holes and alignment grooves etched at the plate edges were designed to hold the plates to within a 0.07-mm registration tolerance.

To vary the angle of view, the collimator plates were

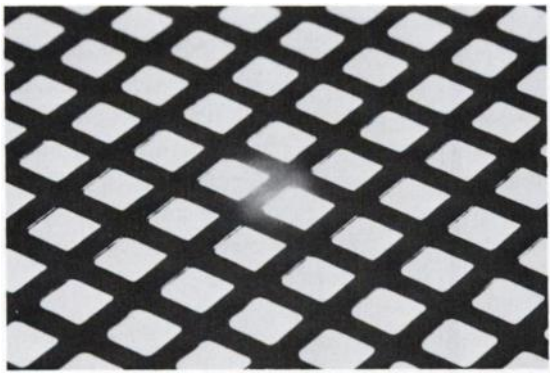

FIG. 2. Microphotograph of typical section of collimator plate. Note regular hole characteristics and mild undercut at hole edges.

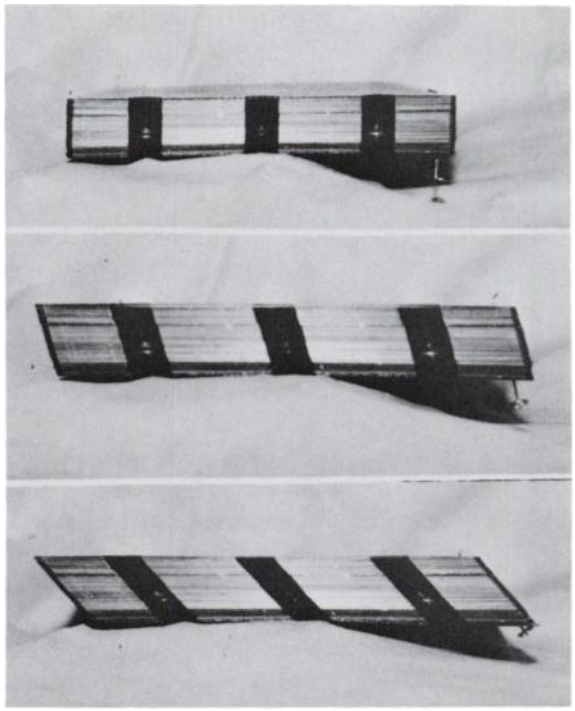

FIG. 3. Side view of VASH collimator "stack" at three shear angles. Note alignment grooves for plate registration.

"sheared" (Fig. 3). Lateral (across the direction of shear) alignment was maintained by two steel retaining walls, within which the plates slid. This design was selected to ensure that plate misregistration and misalignment would not exceed the spetal bar thickness in the maximally sheared position (worst case). The collimator thickness (determined by the number of plates stacked together) was selected to provide, unsheared, a length-to-width ratio that would generate an image spatial resolution similar to that of the conventional GAP collimator. However, other thicknesses can be readily formed by changing the number of plates in the stack. The hard, smooth tungsten surfaces slid easily upon each other and were easily controlled by a parallelogram ram assembly.

The resolution and sensitivity of the collimator were determined with the use of a glass capillary tube (length 70 mm, i.d. 1.24 mm, o.d. 1.6 mm) containing 0.5 μCi pertechnetate (Tc-99m) in water. The thin source was fixed at 5 cm above the collimator while images were recorded using a standard-field scintillation camera with NaI crystal 1.25 cm thick. An energy window of 20% was centered at 140 keV. The data were recorded by a nuclear medical computer system in a manner that yielded an effective matrix element size of 0.6 × 0.6 mm for the central portion of the camera field (zoom mode: 256 × 256 pixels). The pixel size was calibrated in both the x and y directions to permit measurement of the line-spread function full width at half maximum, (FWHM) over a range of slant angles. The calibration of linear

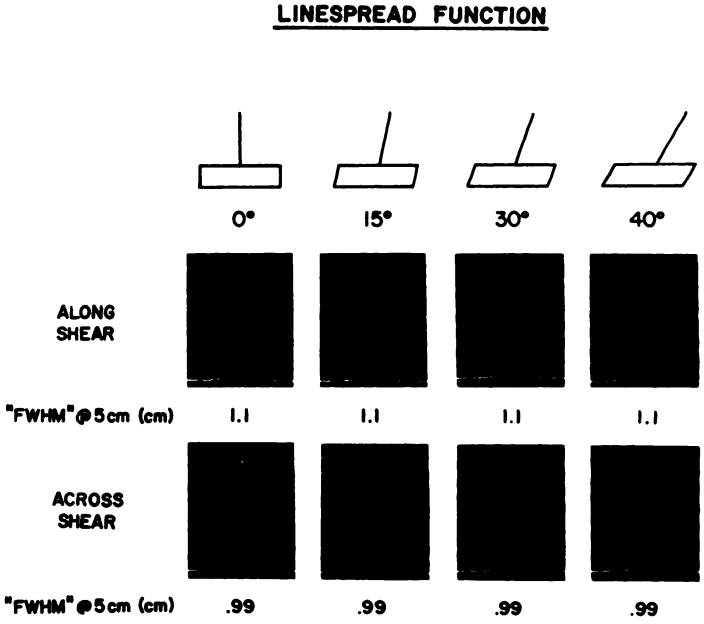

FIG. 4. Pixel position versus counts per pixel: system response to line source with source oriented along and across direction of shear.

dimension to pixel size was used to calculate FWHM in centimeters. Both line-spread functions and sensitivity were then measured at increasing slant angles of 0° (unsheared), 15° (equivalent to 15° slant hole), 30°, and 40° from vertical, moving the line source each time to keep it centered in the field of view. Five-minute images were collected at each angle. The measurement was made both with the line source oriented across the direction of shear and parallel with it.

Relative and absolute sensitivity measurements were made in air, with a single Tc-99m point source located 7.0 cm from the face of the collimator. Data were collected for 60 sec at 0°, 15°, 30°, and 40° with the variable slant-hole collimator, and also with the GAP and high-resolution collimators. The amount of activity in the source was determined in a clinical radionuclide dose calibrator.

RESULTS

The line-spread function taken in bands 5 pixels (3 mm) wide across the axis of the line source, and the FWHM at each angle, are shown on Fig. 4. For the "along shear" measurement, the peak counts declined for increasing angles of shear, to approximately 80% of the unsheared maximum counts. The curves appear continuous and smooth but not necessarily Gaussian in shape.

Using a 20% window, sensitivity was found to be 169 cps/MBq (6.24 cps/μCi) at 0°, 134 cps/MBq (4.96 cps/μCi) at 15°, 65.5 cps/MBq (2.38 cps/μCi) at 30°, and 50.0 cps/MBq (1.84 cps/μCi) at 40° slant angle. For comparison, the sensitivity of the high-resolution collimator was measured as 165 cps/MBq (6.11 cps/μCi) and that of the GAP collimator as 205 cps/MBq (7.58 cps/μCi) (Table 1).

A representative ungated blood-pool image was aquired on a gamma camera at a slant angle of 15°; it shows a resolution similar to that of a GAP (collimator (Fig. 5).

TABLE 1. POINT SOURCE SENSITIVITY RELATIVE TO BOTH GAP AND HI-RES COLLIMATORS AT INCREASING ANGLES OF COLLIMATOR SHEAR

	0°	15°	30°	40°
Relative to GAP	.80	.65	.32	.24
Relative to Hi-RES	1.0	.80	.39	.30

DISCUSSION

Anger's formula (*16*) predicts that for a given septal thickness and source-to-collimator distance, the length-to-width ratio of collimator channels determines the geometric contribution to the line spread function

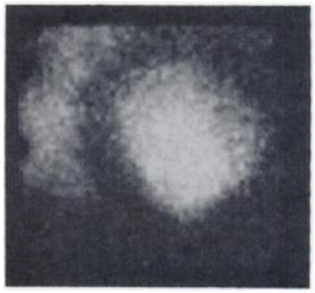

FIG. 5. Ungated blood-pool image (LAO) taken at collimator shear of 15°.

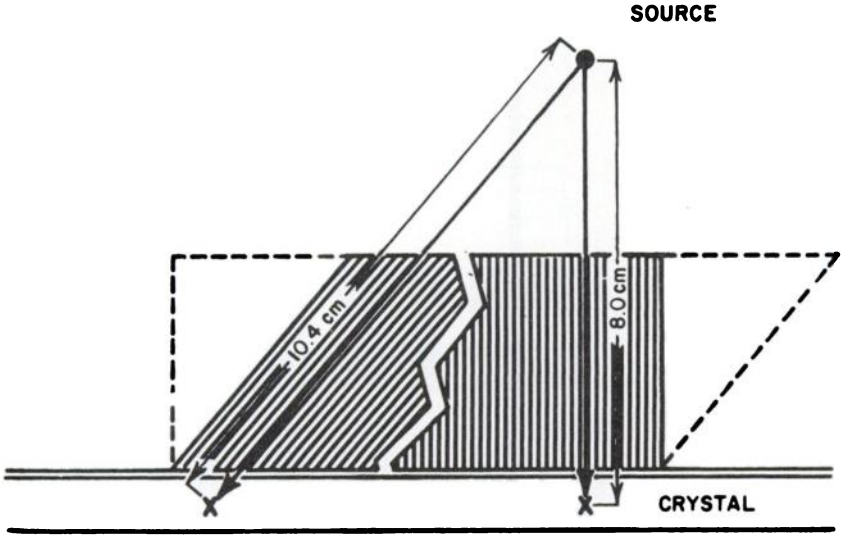

FIG. 6. Schema illustrating changes in hole length and source-to-detector distance that occur when VASH collimator is sheared to 45°.

according to the relation:

$$R_g = d\,(a_e + b + c)/a_e \text{ given } a_e = a - 2\mu^{-1}$$

where a_e = effective collimator height,
a = actual (measured) collimator height,
b = source-to-collimator distance,
c = collimator to crystal's mean depth of interaction,
d = hole diameter,
μ = linear absorption coefficient,
R_g = geometric FWHM.

The calculated geometric resolution at a source-to-collimator distance of 5 cm is 8.21 mm FWHM. The experimental resolution varied from 10 to 11 mm FWHM. If one supposes that the intrinsic resolution for this camera is 6 mm FWHM, then the result is in reasonable agreement with Anger's formula.

Our experimental prototype has relatively thick septa to avoid potential plate-to-plate registration problems. Because the channels become rectangular when the collimator is sheared to increasing angles, one would expect the width of the line-spread function (LSF) to become anisotropic at greater angles of slant, staying constant when measured across the direction of shear but decreasing when measured along the angle of shear. Thus, the FWHM should be proportional to the amount of hole inclination. Since hole length also increases with increasing shear, one expects an improvement in global resolution in both direction from this effect (Fig. 6). One explanation of this finding can be found in the relationship of the source to the collimator holes axes: with increasing slant the distance between the source and detector is increased. However, the LSF width held approximately constant for the range of measurements made. Therefore, the hole lengthening, with corresponding increase in resolution that one expects to see, was probably offset by the decrease in resolution due to the lengthened source-to-detector distance of the angled photon path: the path is inclined and resolution should be degraded by an increased path length alone. Also, higher angles of photon impingement have the effect of spreading the FWHM by travelling across, as well as into, the crystal. The relatively undiminished peak heights of the "ALONG SHEAR" orientation relative to the "ACROSS SHEAR" are probably due to the increasingly rectangular hole shape at increasing angles of shear.

Measured sensitivity at 0° of angulation was less than that of the GAP collimator after which our hole size was patterned. Increased septal thickness lowered the sensitivity to approximately that of a high-resolution collimator.

A close approximation to the sensitivity of a parallel-hole collimator is given by Anger's (*16*) sensitivity formula:

$$\text{Cpm}/\mu\text{Ci} = 2.2 \times 10^6 \times e \times f_a \times k^2 d^4/a_e^2(d + t)^2$$

where:

e = efficiency of camera including window,
f_a = abundance of primary photon,
k = a factor determined by hole shape (0.282 for square holes, 0.238 for round holes)
d = hole diameter
a_e = collimator thickness (effective)
t = septal thickness

When calculated for the unsheared VASH, the result of 169.5 cps/MBq (6.27 cps/μCi) agrees well with the measured point-source sensitivity of 169 cps/MBq (6.24 cps/μCi). Thicker septa (0.8 mm) than in the GAP collimator (0.25 mm) account for the somewhat reduced sensitivity of the VASH compared with the GAP's 205 cps/MBq (7.58 cps/μCi).

Point source sensitivity should decrease as slant angle is increased, due to the shrinkage of the field size, given a consistent amount of intervening absorber and an in-

creasingly tall set of septa. The measured sensitivity decreased faster than the Anger expression predicts. This may be due to faulty registration of the plates at high angles of shear, where registration becomes more critical because of potential septal penetration and irregularity of hole shape. Both must be avoided to ensure predicted performance. The greater-than-predicted falloff in sensitivity suggests that septal penetration was unlikely. Rather, minor irregularities of hole shape could be responsible for reduced collimator sensitivity.

During the design phase, we felt that interplate friction would be a significant problem, but this has not been the case. Tungsten metal is hard enough that the surfaces seem to slide as if lubricated. Currently angulation is set with a parallelogram ram assembly, which works on the plate edges. The surface of the ram plate assembly is chrome-plated to reduce pitting and scratching from the repeated shear motions that occur between the sharp sheet edges and the ram assembly. Future versions may use a knife-edge "racking" mechanism to distribute alignment forces better. Lateral alignment rails received minimum wear: they are primarily guides, and thus experience lower pressure. No significant wear was noted during our short test period. The design is not mechanically complex, and so should be durable. There are alternatives to pure tungsten plates for laminar collimator construction, such as photo-etched lead alloy mounted within Teflon frames. Lead alloys are easily photo-etched, and inexpensive relative to tungsten.

CONCLUSION

The data from this study support the concept that a parallel-hole collimator with adjustable angle of slant can be constructed readily. The collimator does not have marked changes in resolution with angle, but loses approximately 80% of its point-source sensitivity when changed from 0° to 45°. Although the collimator can be sheared to angles greater than 45°, sensitivity will decrease precipitously with angles of photon entry greater than 45°. Future versions with improved plate alignment and thinner septa should not lose sensitivity as quickly as the prototype does as shear angle is increased.

ACKNOWLEDGMENTS

Supported in part by USPHS: NIH Ambulatory Monitoring of Ventricular Function HL24623 and Antimyocin and Ischemia and Infarction HL21751.

REFERENCES

1. SWAN S, PALMER D, KAUFMAN L, et al: Optimized collimator for scintillation cameras. *J Nucl Med* 17:50-53, 1976
2. KIRCOS LT, LEONARD PF, KEYES JW: An optimized collimator for single photon computed tomography with a scintillation camera. *J Nucl Med* 19:322-323, 1978
3. FREEDMAN GS: Gamma camer tomography theory. *Radiology* 102:365-369, 1972
4. CHANG W, LIN SL, KENKIN RE: Multisegmental collimator tomography. In *Emission computed tomography, single photon approach.* Paros P, Eikmans E, Eds. Proceedings of Radiologic Health Symposium, U.S. Gov. Printing Office 1981, pp 65-81.
5. MUEHLLEHNER G: Rotaring collimator tomography. *J Nucl Med* 11:347, 1970 (abst)
6. BUDINGER TF, GULBERG GT: Three dimensional reconstruction in nuclear medicine emission imaging. IEEE Transactions of Nuclear Science NS-21 (3):2-20, 1974
7. GOODWIN PN: Recent developments in instrumentation for emission computed tomography. *Semin Nucl Med* 10: 322-334, 1980
8. MCAFEE JG, MOZLEY JM, STABLER EP: Longitudinal tomographic radioisotopic imaging with a scintillation camera: Theoretical considerations of a new method. *J Nucl Med* 10:654-659, 1969
9. FREEDMAN GS: Tomography with a gamma camera. *J Nucl Med* 11:602-604, 1970
10. MUEHLLEHNER G: A tomographic scintillation camera. *Phys Med Biol* 16:87-96, 1971
11. ROYAL HD, PARKER JA, KOLODNY GM: Noncardiac applications of the slant hole collimator. *J Nucl Med* 22:34, 1981
12. PAVEL DG, MEYER-PAVEL C, MESS D, et al: Rotating slant hole tomography of the hip. *J Nucl Med* 22:27, 1981
13. CHANG W, LIN SL, HENKIN RE: Long axis alignment in collimator tomography of the heart. *J Nucl Med* 22:P66, 1981
14. RATIB O, HENZE E, SCHELBERT HR: Effect of positioning on detection of myocardial perfusion abnormalities by the rotating slant hole collimator. *J Nucl Med* 22:66, 1981
15. CHANG W, LIN SL, HENKIN RE: A study demonstrating that the heart is the only suitable organ for collimator tomography. *J Nucl Med* 22:P34, 1981
16. ANGER HO: Scintillation camera with multichannel collimators. *J Nucl Med* 5:515-531, 1964